Effects of La dilution on the $CePt_2Si_2$ Kondo lattice

F C Ragel[1,#] P de V du Plessis[1,2] and A M Strydom[2]

[1] School of Physics, University of the Witwatersrand, Private Bag 3, PO WITS 2050, Johannesburg, South Africa

[2] Physics Department, University of Johannesburg, P.O. Box 524, Auckland Park 2006, South Africa

E-mail: pdevduplessis@uj.ac.za

Abstract. Electrical resistivity $\rho(T)$ and magnetoresistivity (MR) measurements are presented for the $(Ce_{1-x}La_x)Pt_2Si_2$ alloy system. $\rho(T)$ data at low temperatures for alloys in the concentrated Kondo lattice regime $0 \leq x \leq 0.2$ conform to a $\rho(T)=\rho_0+AT^2$ dependence and Fermi-liquid parameters A and T_{coh} are presented. The maximum that characterize $\rho(T)$ in the concentrated Kondo lattice regime, $T_{max}(\propto T_K)$, is no longer observed for samples with $x \geq 0.3$ which shows single-ion Kondo behaviour. MR measurements on alloys with x=0.5, 0.7 and 0.9 yield values of the Kondo temperature T_K through the Schlottmann analysis. The dependence of A, T_{max} and T_K on x are discussed in terms of the volume and Kondo-hole effects occurring upon alloying. An anomaly, probably of structural origin, in $\rho(T)$ for $LaPt_2Si_2$ and some of the alloy samples are also reported.

1. Introduction

A fascinating modification of the Kondo lattice is the depletion of the local moments by replacing magnetic with nonmagnetic rare-earth ions. There have been numerous experimental studies on such systems [1–6] and the tuning of it between the dense Kondo and single-impurity regimes by doping the f-ion sites with nonmagnetic La, Y or Sc. The non-magnetic impurities in a Kondo lattice are called Kondo holes (see ref. [7]) and an interesting aspect in such Kondo-hole systems is the study of the dependence of transport and thermodynamic properties on the hybridisation resulting from both dilution and volume effects. In this study effects of dilution by La on the $CePt_2Si_2$ Kondo lattice is investigated.

The properties of the parent compound $CePt_2Si_2$ are well documented as being a Kondo lattice compound with no magnetic order down to 0.06 K [8–18]. $CePt_2Si_2$ crystallises in a tetragonal structure, but some differences in interpretation exist regarding its appropriate space group, which is indicated to be the *P4/nmm* $CaBe_2Ge_2$ type [8–11] or a new $CePt_2Si_2$ type of structure [12]. The electrical resistivity $\rho(T)$ of polycrystalline $CePt_2Si_2$ shows a Kondo-like logarithmic increase up to a maximum at T_{max} = 76 K upon cooling and then a steep decrease towards low temperatures [9]. Magnetic susceptibility measurements on polycrystalline $CePt_2Si_2$ show a normal Curie-Weiss behaviour above 150 K with a large negative paramagnetic Curie temperature (θ_P= –86 K). Upon further cooling a broad maximum in $\chi(T)$ is observed around 60 K and an almost constant value is attained below 20 K [9, 13, 14]. Measurements on $CePt_2Si_2$ single-crystals show the strong effects of anisotropy on the magnetisation [14] and electrical resistivity [15, 16]. The ratio of specific heat to temperature C/T drops linearly down to 4 K where the electronic specific heat

[#] On leave from the South Eastern University of Sri Lanka, Oluvil, Sri Lanka.

coefficient γ has a value of 70–86 mJ $K^{-2}mol^{-1}$ [9, 13, 17] below which C/T departs strongly from linearity, turning up to reach a maximum of 120 mJ K^{-2} mol^{-1} at 2 K [9, 17]. While the specific heat [13, 17] and resistivity [13] exhibit Fermi-liquid behaviour between 4 and 10 K, measurements of specific heat and electrical resistivity below 4 K suggest non-Fermi-liquid behaviour [13, 17].

Previous alloying studies on $CePt_2(Si_{1-x}Ge_x)_2$ [19], $Ce(Pt_{1-x}Ni_x)_2Si_2$ [20] and $CePt_2(Si_{1-x}Sn_x)_2$ [21] ligand systems, as well as a study on a limited number of $(Ce_{1-x}La_x)Pt_2Si_2$ alloys [22] have been interpreted in terms of the effect of the volume changes induced by chemical pressure in these alloys on the Kondo parameters by invoking the compressible Kondo lattice model [23, 24]. The present much more detailed study of $\rho(T)$ and which is also extended to include magnetoresistance (MR) measurements of the $(Ce_{1-x}La_x)Pt_2Si_2$ system enables us not only to interpret the results in terms of volume effects, but also to include the effects due to dilution (Kondo holes) in our description of the results. In addition, anomalous behaviour of $\rho(T)$ is found in the present study which was not uncovered by the authors of reference [22].

2. Experimental

Polycrystalline samples of $(Ce_{1-x}La_x)Pt_2Si_2$ $(0 \le x \le 1)$ were prepared by arc-melting stoichiometric amounts of the constituent elements on a water-cooled copper hearth in a titanium gettered ultra high purity inert argon gas atmosphere. The purities in wt% of the materials used were Ce: 99.98, La: 99.99, Pt: 99.97 and Si: 99.999. A weight-loss of less than 0.5% was observed during melting for all alloys.

X-ray powder diffraction measurements on the $(Ce_{1-x}La_x)Pt_2Si_2$ alloys ascertained the phase purity of the samples and the absence of unreacted elements. The lattice parameters a and c of the tetragonal compounds were calculated using standard regression analysis of 22 well-resolved peaks of the powder spectrum of each alloy.

The temperature dependent electrical resistivity $\rho(T)$ was measured using a standard dc four-probe technique in the temperature range 4–300 K on bar-shaped samples of typical dimension 8 x 1 x 1 mm^3 cut by spark-erosion. Temperatures were measured using a Au–0.07 at. % Fe versus chromel thermocouple with an absolute accuracy of $T \pm 0.5$ K. Magnetoresistance measurements have also been performed on selected alloys in fields up to 8 T.

3. Results and discussion

3.1 X-ray diffraction analysis

Powder XRD results indicate a tetragonal structure for all compositions of the $(Ce_{1-x}La_x)Pt_2Si_2$ system. However, our powder diffraction data cannot distinguish between the $CePt_2Si_2$ type [12] and $CaBe_2Ge_2$-type [8–11] structures since the additional reflections $(h\,k\,0)$ with $h+k=2n+1$ appearing in the $CePt_2Si_2$ type are very faint and are discernible only from single crystal data according to reference [12]. Our powder XRD results are therefore analysed on the basis of the tetragonal $CaBe_2Ge_2$-type structure. Lattice parameters a and c, c/a and the unit-cell volume of the alloy series are shown in figure 1. It is observed that the parameters a and c and the unit-cell volume increase linearly with x following Vegard's rule and the c/a ratio decreases with increasing x. The determined room-temperature tetragonal lattice parameters of $CePt_2Si_2$, viz. a=4.253(2) x 10^{-1} nm, c=9.793(4) x 10^{-1} nm and the crystallographic unit-cell volume V=177.2(2) x 10^{-3} nm^3 are in agreement with the literature [9, 11]. The corresponding structural parameters obtained for the $LaPt_2Si_2$ alloy are a=4.286(1) x 10^{-1} nm, c=9.823(2) x 10^{-1} nm and V=180.4(1) x 10^{-3} nm^3, which are also consistent with data reported by Gignoux *et al* [9].

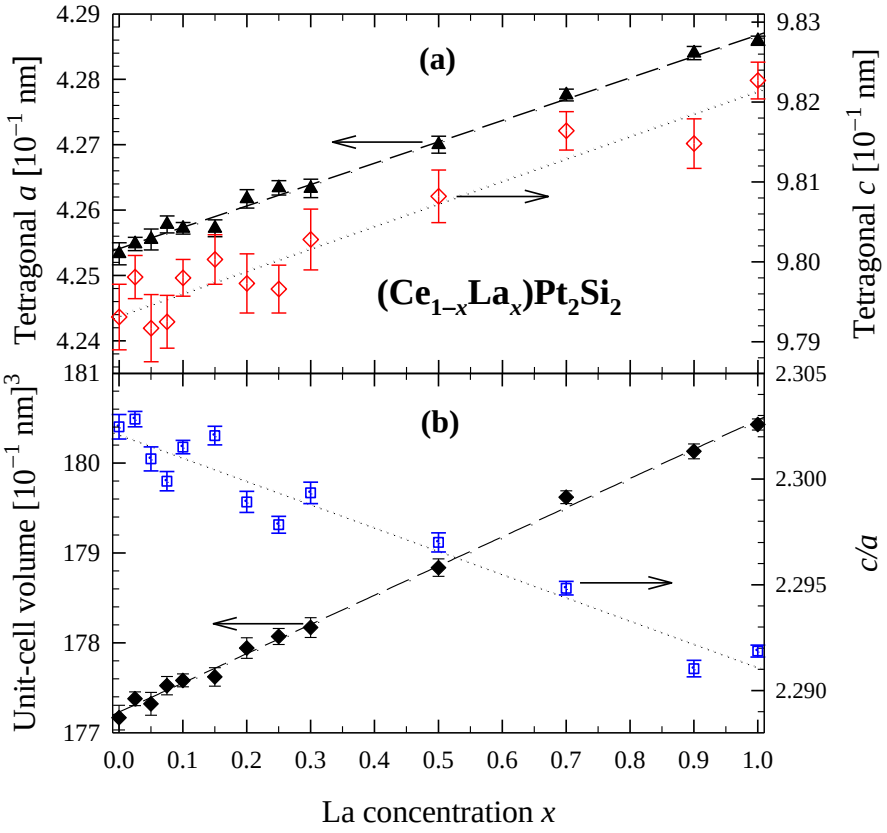

Figure 1. The tetragonal lattice parameters (a) a and c, (b) the unit-cell volume V and the ratio c/a of alloy compositions $0 \le x \le 1$ of the $(Ce_{1-x}La_x)Pt_2Si_2$ system.

3.2 Resistivity measurements

The $\rho(T)$ measurements as a function of temperature on as-cast samples of the $(Ce_{1-x}La_x)Pt_2Si_2$ alloys are shown in figure 2 which illustrates a transition from the dense Kondo regime ($0 \le x \le 0.25$) through the single-ion Kondo regime ($0.3 \le x \le 0.9$) to metallic behaviour (x=1). A well-resolved anomalous kink in $\rho(T)$ is evident in figure 2(b) for $LaPt_2Si_2$, as well as in some of the other alloys and this phenomenon will be discussed in section 3.2.2. In the dense Kondo regime, single-ion Kondo scattering dominates at higher temperatures and the $\rho(T)$ curves initially display a logarithmic upturn upon cooling. Subsequently $\rho(T)$ goes through a maximum at temperature T_{max} as a result of coherence effects, and further cooling gives rise to Fermi-liquid behaviour which is shown in figure 3. As illustrated in the insert in figure 2, T_{max} decreases from 64.4 K for x=0 to 15.5 K for x=0.25, extending the single-ion Kondo scattering region to lower temperatures. The solid lines in figure 3 are linear least-squares (LSQ) fits of the relation $\rho(T)=\rho_0 + AT^2$ (ρ_0 is the residual resistivity) to the data below the coherence temperature T_{coh}, the results of which are given in table 1. The determined value $A = 0.079 \times 10^{-8}\ \Omega\,m\,K^{-2}$ for $CePt_2Si_2$ is in good agreement with previous observations [13, 22].

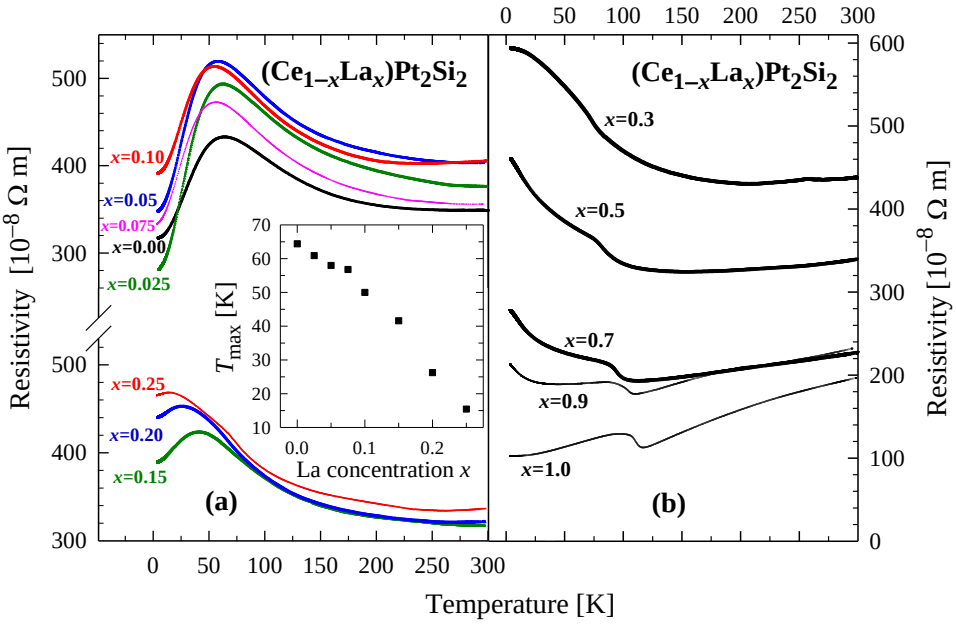

Figure 2. Dependence of the resistivity on temperature for the alloy compositions $0 \leq x \leq 1$ of the $(Ce_{1-x}La_x)Pt_2Si_2$ system. The insert shows the T_{max} dependence on x.

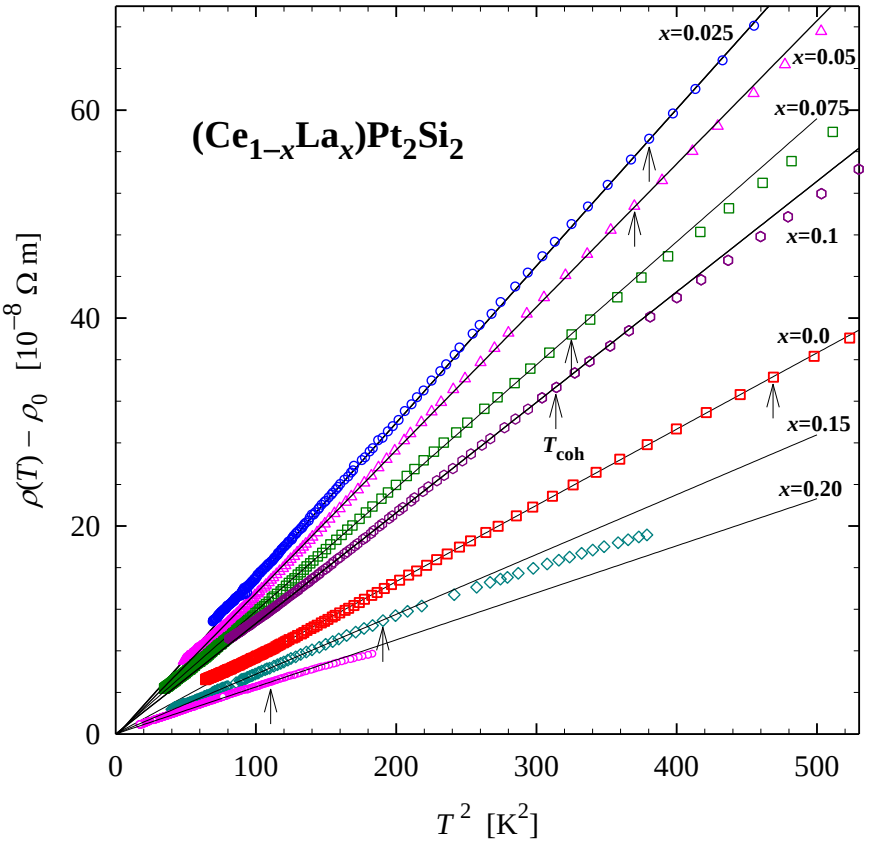

Figure 3. Fermi-liquid T^2 behaviour of the resistivity for the $(Ce_{1-x}La_x)Pt_2Si_2$ alloys with $0 \leq x \leq 0.2$. The arrows refer to the onset of the T^2-dependence and hence to T_{coh} of each alloy. T_{coh} has been taken as the highest temperature point of which the linear relationship between $\rho(T)-\rho_0$ and T^2 is still evident.

Table 1. Results of LSQ fits of the relation $\rho(T)=\rho_0+AT^2$ to the $\rho(T)$ data in figure 3.

x	T_{coh} [K]	A [10^{-8} Ω m K^{-2}]	ρ_0 [10^{-8} Ω m]
0.00	21.7	0.0787(1)	337.04(2)
0.025	19.5	0.1509(2)	277.09(3)
0.050	19.7	0.1366(3)	344.21(3)
0.075	18.4	0.1182(2)	329.28(2)
0.10	17.4	0.1428(4)	387.57(4)
0.15	13.8	0.0575(2)	388.56(1)
0.20	10.5	0.0452(1)	439.65(1)

3.2.1 *Dilution effect.* The interplay between dilution and volume effects on the Fermi-liquid parameters A and T_{coh} is discussed by comparing these parameters for $(Ce_{1-x}La_x)Pt_2Si_2$ ($0\le x\le 0.2$) with those obtained for $Ce(Pt_{1-y}Ni_y)_2Si_2$ ($0\le y\le 0.5$) [20] in figures 4 and 5. It is seen from figure 4 that A increases with a decrease in y and hence increase in volume for the $Ce(Pt_{1-y}Ni_y)_2Si_2$ series. This result is in agreement with pressure studies on $CePt_2Si_2$ which show a rapid decrease in A with pressure [13] and hence an increase in A with increase in volume. Similar results are also obtained for $CeCu_2Si_2$ [25], UBe_{13} [26], $CeInCu_2$ [27] and Ce_7Ni_3 [28] through hydrostatic pressure studies. The results for the $(Ce_{1-x}La_x)Pt_2Si_2$ system show a large increase in A with increase in volume for the x=0.025 alloy with respect to the x=0 parent compound (table 1 and figures 4 and 5). This result is in agreement with the pressure studies mentioned earlier [13]. All the preceding results are considered as due to the dominance of volume effects in the behaviour of the A coefficient. However, A of $(Ce_{1-x}La_x)Pt_2Si_2$ shows a decrease with further increase in x and this is considered as due to the dominance of the dilution effect over the volume effect as may be motivated by considering the theoretical predicted properties of Kondo hole systems [7, 29, 30]. Substituting Ce by non-magnetic Kondo holes gradually smears out the hybridisation (pseudo) gap, which is formed around the renormalized f-level position. Hence the gradual substitution of Ce with La to form Kondo holes results in a gradual diminishing of the coherence thus causing a decrease in A and in T_{coh} as the f-electron density of states gradually changes from a two-peak coherent state to a single-peak incoherent state [29, 30]. A decrease in A with increase in La concentration and hence volume is also observed in several La based systems such as $(Ce_{1-x}La_x)Cu_2Si_2$ [31], $(Ce_{1-x}La_x)Cu_6$ [32] and $(Ce_{1-x}La_x)Ni_9Si_4$ [33] and may thus also be interpreted as due to the dominance of the Kondo-hole effect over the volume effect. Furthermore, the behaviour of $\gamma(\propto\sqrt{A})$ for the $(Ce_{1-x}La_x)_3Al$ system which shows a maximum around x=0.6 [34] is considered to arise due to the competing interplay of these two effects. Theoretical calculations based only on Kondo hole substitution without reference to a volume contribution predict a decrease in A [35]. Turning the attention to T_{coh}, it is noted that it is expected to decrease with increase in volume (negative pressure) [25–28] as is also seen for the $Ce(Pt_{1-y}Ni_y)_2Si_2$ system in figure 4. However, an additional contribution to the decrease of T_{coh} due to dilution is evident for the $(Ce_{1-x}La_x)Pt_2Si_2$ alloys.

Figure 6 illustrates the evolution from the Kondo lattice regime through the single-ion Kondo regime to metallic behaviour with increased La concentration. One observes the destruction of coherence as the periodicity of the Ce sublattice is destroyed by the substitution of La, which suppresses the drop of $\rho(T)$ at low temperatures. The gradual destruction of coherence in the Kondo lattice can be well illustrated by subtracting $[\rho_{x=0}(T)-\rho_{x=0}(0)]$ of $CePt_2Si_2$ from $\rho_x(T)$ of the dense Kondo ($0.025\le x\le 0.1$) alloys as shown in the insert in

figure 6. It is seen that the relative drop in $\delta\rho(T)/\delta\rho(150\,\mathrm{K})$ decreases and attains a higher $\delta\rho(4\,\mathrm{K})/\delta\rho(150\,\mathrm{K})$ value with a small increase in La concentration.

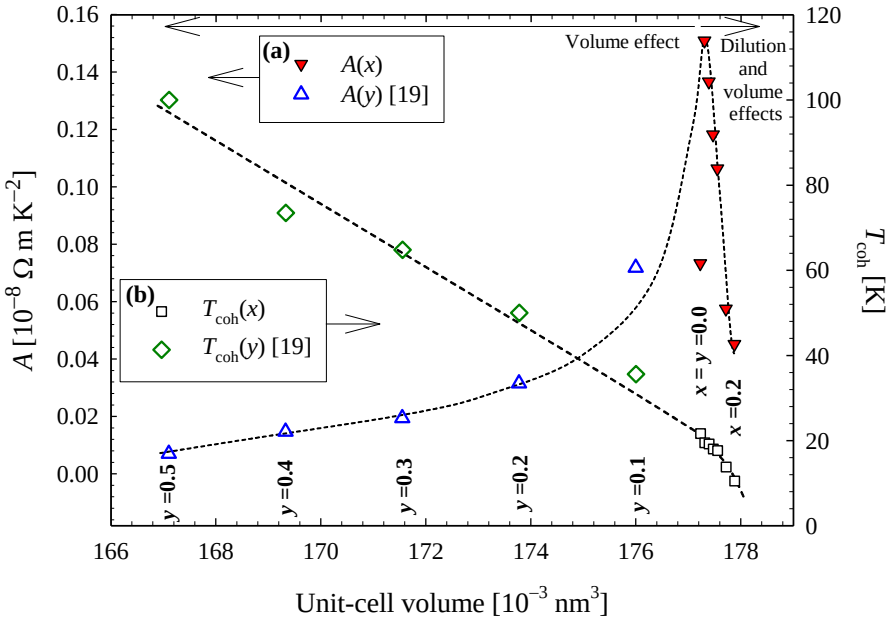

Figure 4. Fermi-liquid parameters A and T_{coh} of $(Ce_{1-x}La_x)Pt_2Si_2$ and $Ce(Pt_{1-y}Ni_y)_2Si_2$ [20] systems are plotted against unit-cell volume. The dashed curves are a guide for the eye. Volume dependence of (a) the T^2 coefficient A of $\rho(T)$ (L.H.S. scale); (b) the temperature T_{coh} below which the T^2 behaviour of $\rho(T)$ is observed (R.H.S. scale). The contribution of volume and dilution effects on compositions $0 \le x \le 0.2$ are compared with the results of compositions $0 \le y \le 0.5$ for which only a volume effect is indicated.

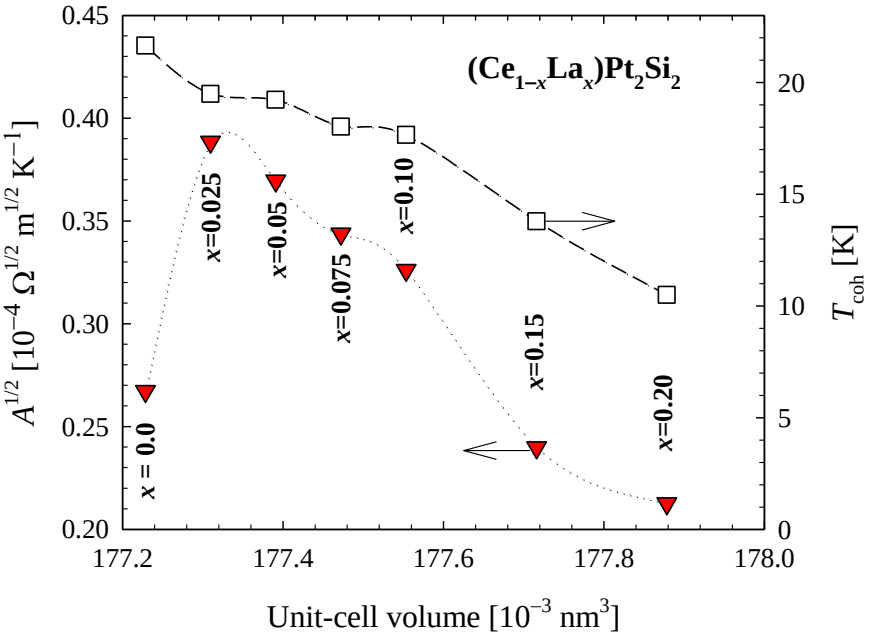

Figure 5. Plot of $A^{1/2}(\propto \gamma)$ and T_{coh} against unit-cell volume of $(Ce_{1-x}La_x)Pt_2Si_2$ $(0 \le x \le 0.2)$. The curves are a guide for the eye.

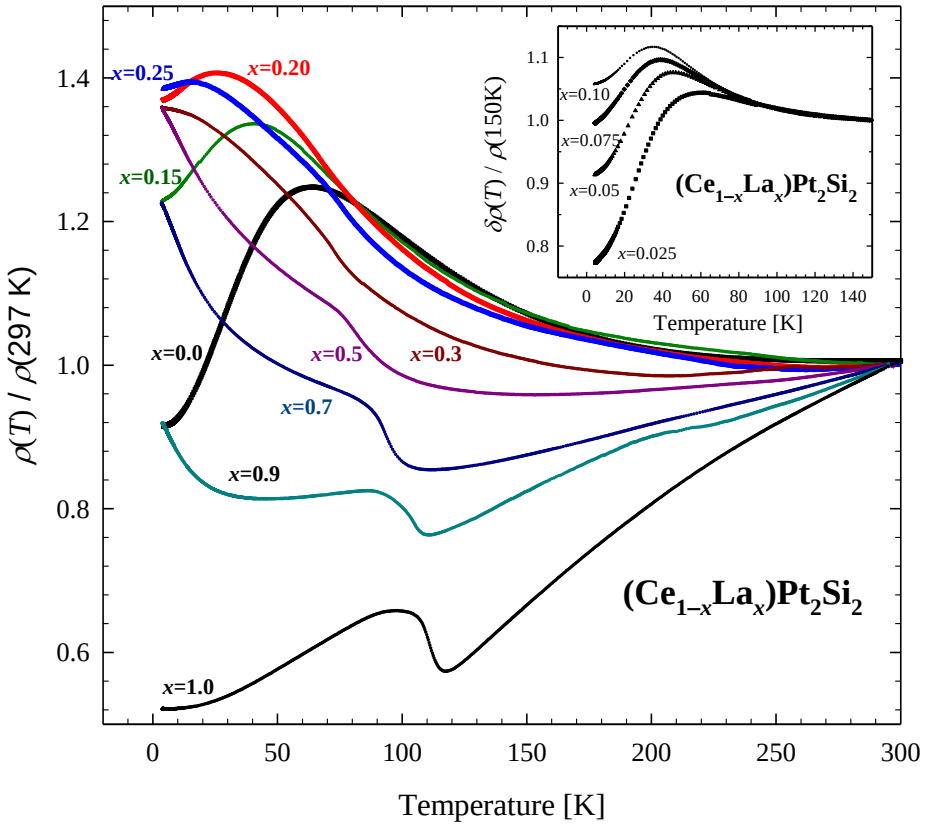

Figure 6. Plot of $\rho(T)/\rho(297\ \mathrm{K})$ against temperature which illustrates the evolution from the Kondo lattice regime through the single-ion Kondo regime to metallic behaviour. The insert shows the $\delta\rho_x(T)=\rho_x(T)-[\rho_{x=0}(T)-\rho_{x=0}(0)]$ results of alloys compositions $0.025\leq x\leq 0.1$ normalized to 150 K, which illustrates suppression of coherence with a small amount of La substitution on the $CePt_2Si_2$ Kondo lattice.

Apart from its effect on the Fermi-liquid parameters, an increase in the Kondo hole concentration also decreases the Kondo energy scale T_{max} ($\propto T_K$). This is shown from theoretical studies based only on the dilution effect and not considering the volume effect which indicates that an increase in x extends the incoherent Kondo scattering region to lower temperatures [30, 35, 36]. The gradual change from a two-peak to a single peak density of f–electron states associated with a change from coherent to incoherent behaviour takes place around a characteristic concentration x_c [29]. To provide contact between experiment and theory one may identify x_c with the concentration of La at which T_{max} is just no longer observed upon increased dilution. For the $(Ce_{1-x}La_x)Pt_2Si_2$ system $x_c \approx 0.25$–0.3. The value of x_c as introduced here varies for different Kondo systems as deduced from experimental results in the literature and is as diverse as $x_c \approx 0.03$ for $(Ce_{1-x}La_x)Pd_3$ [37] and $x_c \approx 0.6$ for $(Ce_{1-x}La_x)Cu_2Si_2$ [31]. On the other hand the effect of volume change on T_{max} ($\propto T_K$) in the alloy system is described by the compressible Kondo lattice (CKL) model [23, 24]. With increase in volume due to an increase in La concentration, a decrease in T_{max} is expected (see equation (1) below). Hence, an additional contribution T_{max}^{Kh} due to dilution with La is expected over and above the conventionally considered volume effect. Thus in a Ce-La based system, T_{max} is expected to decrease more rapidly with negative pressure owing to the additional contribution of T_{max}^{Kh}.

Alloying studies on the $Ce(Pt_{1-y}Ni_y)_2Si_2$ system show the dominance of pressure (i.e. volume) effects on T_{max} as compared with other compounds investigated earlier with hydrostatics pressure studies and displayed in figure 10 of ref. [20]. Hence, the ligand system $Ce(Pt_{1-y}Ni_y)_2Si_2$ has been used as a reference for the volume effect in applying the

compressible Kondo lattice (CKL) model [23, 24] to obtain a quantitative measure of T_{max}^{Kh} for the $(Ce_{1-x}La_x)Pt_2Si_2$ system. The CKL model for Ce compounds [23, 24] gives the volume dependence of $|J\,N(E_F)|$ as $|J\,N(E_F)| = |J\,N(E_F)|_0 \exp[-q(V-V_0)/V_0]$, where $|J\,N(E_F)|_0$ indicates the value of the quantity at an initial volume V_0. Furthermore, q refers to the Grüneisen parameter of $|J\,N(E_F)|$ (i.e. $q = -\partial \ln|JN(E_F)|/\partial \ln V$) and it is considered to vary between 6 and 8 [23, 27]. Since $T_{max} \propto T_K \propto \exp(-1/|JN(E_F)|)$ the volume dependence of T_{max} may be described by

$$T_{max}(V) = T_{max}(V_0)\,\exp\left[\frac{q\,(V_0 - V)}{|J\,N(E_F)|_0\,V_0}\right] \qquad (1)$$

as a function of the concentration dependent volume V as done in many such studies in the literature [19, 21, 27, 28]. A similar study of applying (1) to the T_{max} behaviour has been reported for the $Ce(Pt_{1-y}Ni_y)_2Si_2$ system [20]. The data from the latter study are reproduced in figure 7 and a LSQ fit of (1) to the experimental data is shown by the dashed curve and gives $q/|JN(E_F)| = 21.7(2)$. This curve has been extrapolated to the negative pressure region and used as a reference $T_{max}(V_{ref})$ of the volume effect on T_{max} for $CePt_2Si_2$ based systems. Hence, the dilution contribution $T_{max}^{Kh}(x) = T_{max}(V_{ref}) - T_{max}(x)$ has been calculated for the $(Ce_{1-x}La_x)Pt_2Si_2$ $(0 \le x \le 0.25)$ system and plotted in the insert to figure 7. As seen in the insert, T_{max}^{Kh} increases as x approaches the characteristic concentration x_c at which the resistivity peak disappears.

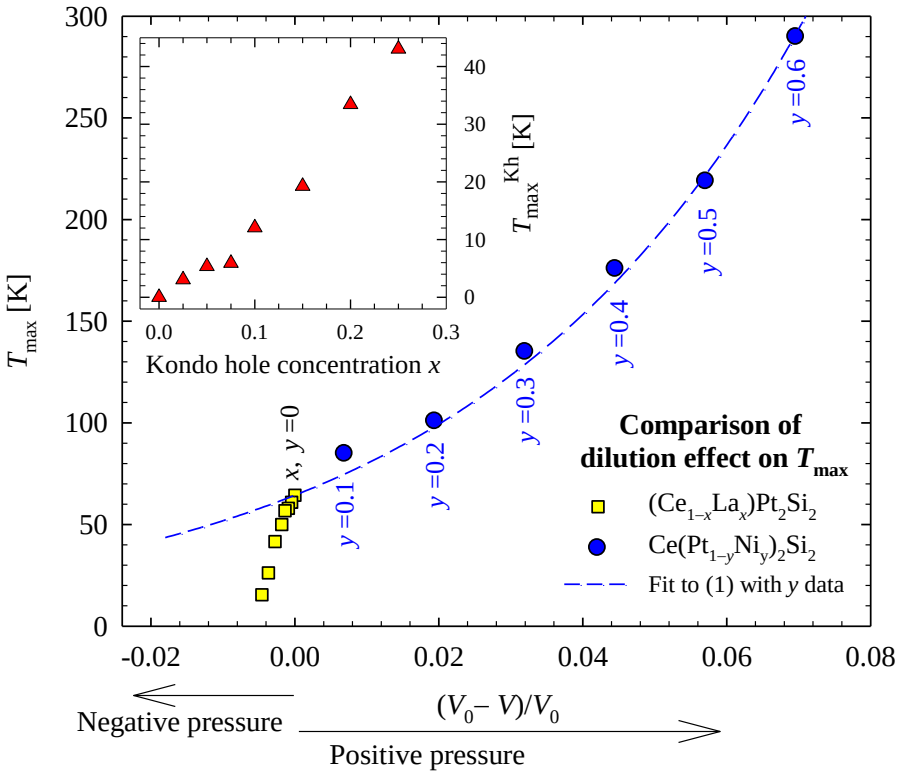

Figure 7. Unit-cell volume dependence of the position of the resistivity maximum T_{max} of the Kondo hole system $(Ce_{1-x}La_x)Pt_2Si_2$ and the ligand system $Ce(Pt_{1-y}Ni_y)_2Si_2$ [20]. The dashed line is the LSQ fit to equation (1) for the $Ce(Pt_{1-y}Ni_y)_2Si_2$ system [20]. The insert shows the x dependence of the dilution contribution $T_{max}^{Kh}(x) = T_{max}(V_{ref}) - T_{max}(x)$.

3.2.2 *Signs of a low-temperature structural change in La rich alloys.* Measurements on bars cut from several different ingots confirm a kink in $\rho(T)$ for the non-magnetic $LaPt_2Si_2$ compound that has not to our knowledge been reported yet. This kink is also seen in other $(Ce_{1-x}La_x)Pt_2Si_2$ alloys in figures 2, 6 and 8, and is shifted towards lower temperatures with the decrease of La concentration. It is shown in figure 8(a) and (b) that there is a marked hysteresis associated with this kink, with the kink occurring at a lower temperature during the cooling run than during the heating run. Similar kinks with hysteresis in the electrical resistivity have been reported by Besnus *et al* [38] in ternary $RInAu_2$ intermetallics with R=La, Ce, Pr and Nd. It has been shown in their work that a phase transition from the high temperature cubic to low temperature tetragonal structure occurs at the transformation temperature T_M. Such anomalies in the resistivity have also been reported in numerous cubic CsCl-type compounds like $LaAg_{1-x}In_x$ [39], $CeAg_{1-x}In_x$ [40] or RCd, where R is a rare-earth element [41]. $LaAg_{1-x}In_x$ and $CeAg_{1-x}In_x$ have the cubic CsCl structure at room temperature and undergo a martensitic transition to a tetragonal phase at low temperatures, which is ascribed to the Jahn-Teller effect [40]. In figure 8(c) it is shown that the transformation temperature T_M increases linearly with unit-cell volume for our $(Ce_{1-x}La_x)Pt_2Si_2$ alloys. As an approximation values of unit-cell volume derived from XRD measurements at room temperature were used in figure 8 since we lacked the facilities to study the temperature dependence of the lattice parameters. Extrapolation of our T_M points shows that such a kink should appear around 62 K in $\rho(T)$ of $CePt_2Si_2$. However, the anomaly is not observed in $CePt_2Si_2$, and since the hysteresis associated with a kink is more prominent in La rich samples, it suggests that the La in the alloy is responsible for this anomaly. Temperature-dependent measurements of the structural parameters of the alloy compositions exhibiting the anomaly are called for to ascertain if a structural phase transition is associated with the anomaly in $\rho(T)$.

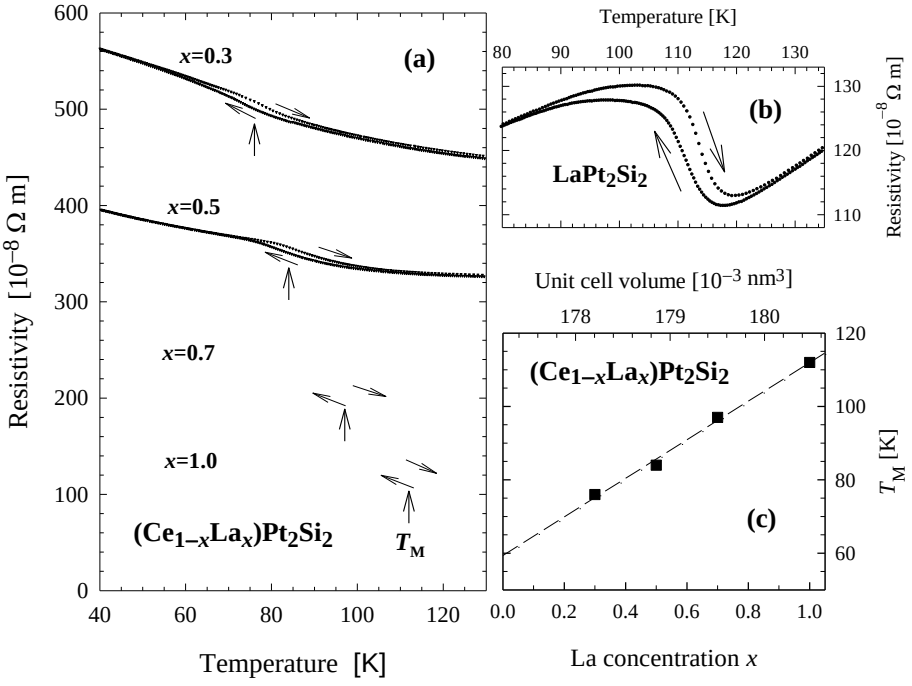

Figure 8. (a) The kink in the $\rho(T)$ data of $(Ce_{1-x}La_x)Pt_2Si_2$ ($0.3 \le x \le 1.0$) alloys and (b) an enlarged figure of the kink in $LaPt_2Si_2$, showing hysteresis between cooling and heating runs. (c) Plot of T_M, the temperature at which a kink with a hysteresis appears (taken approximately at the position with maximum hysteresis of $\rho(T)$) against unit–cell volume and La concentration x of the $(Ce_{1-x}La_x)Pt_2Si_2$ ($0.3 \le x \le 1.0$) alloys, which shows approximately a linear increase of T_M with unit-cell volume.

3.3 Magnetoresistivity measurements

The magnetoresistivity defined as MR=[$\rho(T, \mu_0 H)-\rho(T, 0)$]/$\rho(T, 0)$ was measured for isotherms between 1.5 and 60 K for alloys of composition x=0.5, 0.7 and 0.9 which all are in the single–ion Kondo regime as is evident from figure 6. The MR isotherms were measured in transverse fields $\mu_0 H$ up to 8 T. A typical example of the results is shown in figure 9 for the $(Ce_{0.5}La_{0.5})Pt_2Si_2$ sample. Results taken during increasing fields always fall on the same curve with data taken during decreasing fields. The behaviour in figure 9 is typical of the suppression of the incoherent Kondo scattering in a magnetic field. Except for the isotherm at the lowest temperature of 1.5 K, it is observed that the data are well described by the results of the Bethe ansatz calculations of the Coqblin-Schrieffer model as predicted by Andrei [42] and Schlottmann [43]

$$\frac{\rho(B)}{\rho(0)} = \left[\frac{1}{2j+1} \sin^2\left(\frac{\pi n_f}{2j+1} \right) \sum_{\ell=0}^{2j} \sin^{-2}\left(\pi n_\ell\right) \right]^{-1} . \qquad (2)$$

As discussed in more detail in ref. [20], at low enough temperatures (T<<Δ_{CF}, where Δ_{CF} is the overall crystal field splitting) in systems having T_K<Δ_{CF}, only the ground state crystal-field level is populated and hence at such low temperatures the system behaves as if in spin-$\frac{1}{2}$ state. The overall crystal field splitting in the $CePt_2Si_2$ compound is reported to be $\Delta_{CF} \approx 100$ K [44]. Results of specific heat and susceptibility experiments indicate Kondo temperature T_K ranging from 45 K [9] to 70 K [13] for $CePt_2Si_2$. Hence for the $(Ce_{1-x}La_x)Pt_2Si_2$ ($0.5 \le x \le 0.9$) alloys (since T_K is expected to decrease due to volume and dilution effects as observed in the decrease of T_{max} with increasing x) T_K<Δ_{CF} and as an approximation only the ground state doublet may effectively operate ($j = \frac{1}{2}$) at low temperatures (T<T_K). The solid lines in figure 9 are LSQ fits for the $j = \frac{1}{2}$ case of (2) to the experimental data. The exact solutions for $j = \frac{1}{2}$ in the above model indicate that the MR is completely determined by a single parameter, the characteristic field B* [43], which is expected to have the following temperature dependence [45]

$$B^*(T) = B(0) + \frac{k_B T}{g\mu_K} = \frac{k_B (T_K + T)}{g\mu_K} . \qquad (3)$$

Values of B*(T) obtained from the LSQ fits of (2) to the data in the main figure, are plotted in the insert in figure 9. The linear relation predicted by (3) is borne out at low temperature, but there is some deviation from linearity of the B* value of the 60 K isotherm which may be associated with an increased population of the first excited crystal-field level with increasing temperature. A LSQ fit of (3) to the B*(T) points, yields B*(0), hence T_K, and also the corresponding magnetic moment μ_K of the Kondo ion. Values of T_K and μ_K thus obtained for the investigated alloys are given in table 2. It is shown in figure 10 that all isotherms between 5 and 20 K conform to the universal scaling of B*(T). A related scaling behaviour encompassing both the x=0 and x=0.5 members of the $Ce(Pt_{1-x}Ni_x)Sn$ alloy system has been previously reported [46].

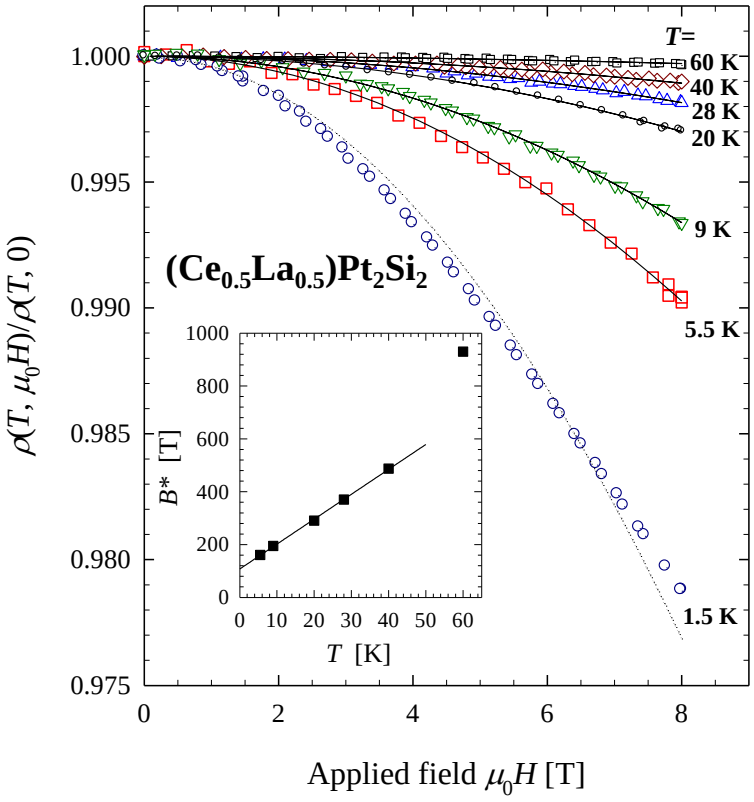

Figure 9. The magnetic field dependence of the electrical resistivity at a number of sample temperatures for the alloy $(Ce_{0.5}La_{0.5})Pt_2Si_2$. The data have been measured in increasing and decreasing fields without evidence of hysteresis. The solid curves in the main figure are LSQ fits of the Bethe ansatz theory of magnetoresistivity equation (2) to the experimental data. The data for the 1.5 K isotherm deviate from equation (2) (depicted as a dotted line). The insert shows the temperature variation of the characteristic field $B^*(T)$, and the solid line is a LSQ fit of equation (3) to the data.

Table 2. Values of the Kondo temperature T_K and the magnetic moment of the Kondo ion μ_K as obtained from LSQ fits of equations (2) and (3) to the MR data of the alloy compositions $0.5 \le x \le 0.9$ of the $(Ce_{1-x}La_x)Pt_2Si_2$ system.

x	0.5	0.7	0.9
T_K [K]	11.4 ± 0.4	5.6 ± 1.0	2.6 ± 0.6
μ_K [μ_B]	0.111 ± 0.002	0.078 ± 0.005	0.039 ± 0.003

In figure 11 the volume dependence of T_{max} obtained from the $\rho(T)$ curves and T_K as deduced from MR measurements on the $(Ce_{1-x}La_x)Pt_2Si_2$ alloys are compared with the CKL model as obtained for the $Ce(Pt_{1-y}Ni_y)_2Si_2$ system (see figure 7) and depicted by a dashed line. It is observed that the T_K values also deviate from the CKL model prediction. This confirms the notion discussed in section 3.2.1 that the Kondo energy scale in $(Ce_{1-x}La_x)Pt_2Si_2$ depends sensitively on both the unit-cell volume and on dilution effects. Theoretical work by Castro Neto and Jones [47] also addresses such distinctions between pressure and dilution effects.

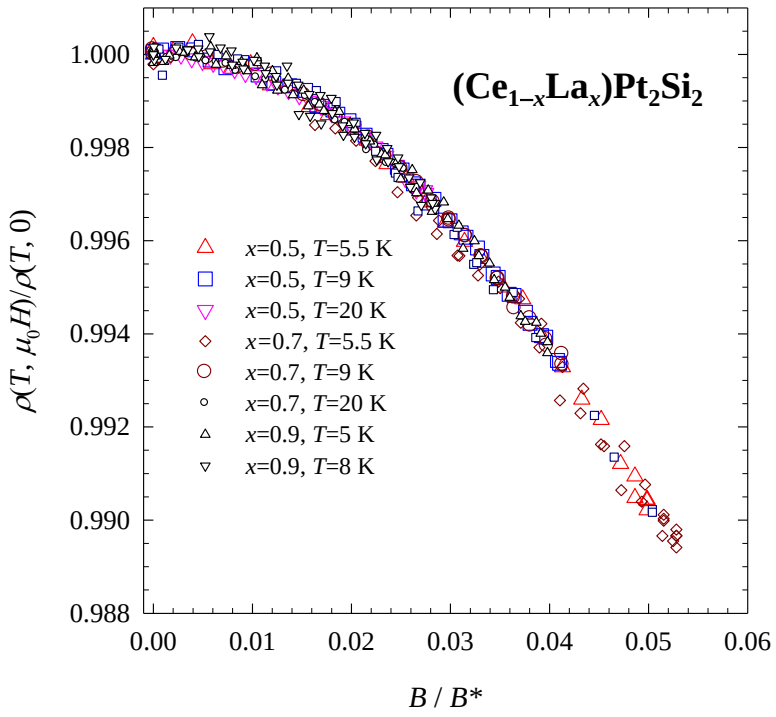

Figure 10. The universal scaling of $B^*(T)$ observed for alloy compositions $0.5 \le x \le 0.9$ of the $(Ce_{1-x}La_x)Pt_2Si_2$ system. Data for isotherms between 5 and 20 K for the concentrations x=0.5, 0.7 and 0.9 all fall on one curve.

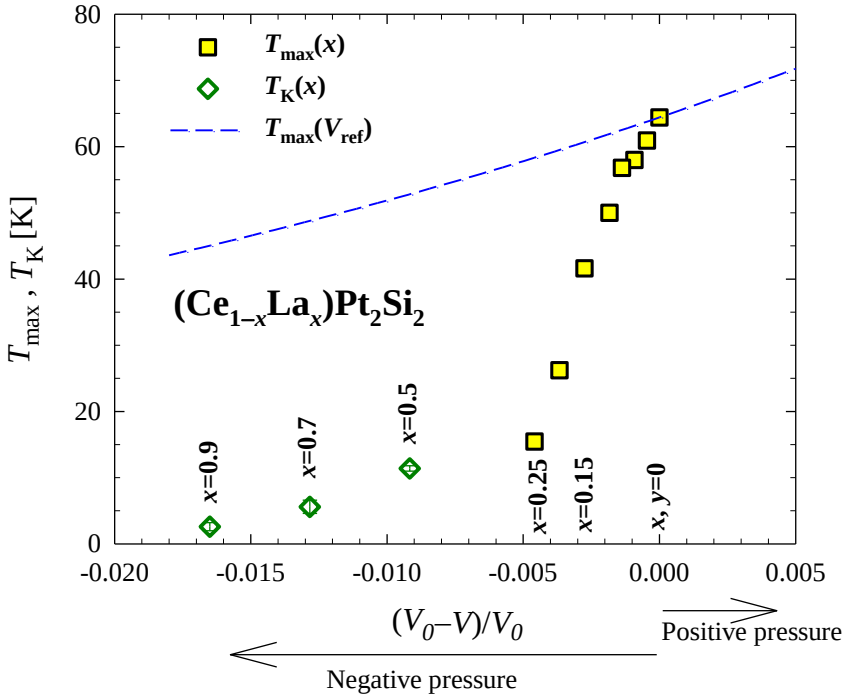

Figure 11. Volume dependence of T_{max} and T_K for the $(Ce_{1-x}La_x)Pt_2Si_2$ ($0 \le x \le 0.9$) system. The fit of equation (1) to the $T_{max}(y)$ values of $Ce(Pt_{1-y}Ni_y)_2Si_2$ (see figure 7) is used as a reference $T_{max}(V_{ref})$ (dashed line) for the approximate volume contribution to the $T_{max}(x)$ behaviour of the $(Ce_{1-x}La_x)Pt_2Si_2$ system.

Conclusion

Resistivity studies on the $(Ce_{1-x}La_x)Pt_2Si_2$ alloy system illustrate the transition from the dense Kondo regime ($0 \le x \le 0.25$) to the single-ion Kondo regime. The behaviour of the Fermi-liquid parameter $A(x)$ in the $\rho(T)=\rho_0+AT^2$ dependence and the position $T_{max}(x)$ of the maximum in $\rho(T)$ in the dense Kondo regime of the alloy system is qualitatively described by considering both volume and Kondo-hole effects. Magnetoresistivity studies in the single-ion Kondo regime are interpreted in terms of the Schlottmann formalism. An anomaly in $\rho(T)$ of $LaPt_2Si_2$ and some of the other alloys is reported and further investigation by other techniques is required to resolve its origin.

Acknowledgements

Support by the South African National Research Foundation (NRF) through grants GUN 2053778 and GUN 2072956 and the Research Division of the University of the Witwatersrand (Wits) is acknowledged. Dr. M. B. Tchoula Tchokonté is thanked for assisting with the x-ray diffraction measurements. F. C. Ragel wishes to thank the NRF and Wits University for granting bursaries for the study, and the University of Johannesburg for funding a recent visit to its Physics Department. He also extends his appreciation to the South Eastern University of Sri Lanka for granting leave to pursue his research in South Africa.

References

[1] Schilling J S 1986 *Phys. Rev. B* **33** 1667; and references therein
[2] Sumiyama A, Oda Y, Nagano H, Ōnuki Y, Shibutani K and Komatsubara T 1986 *J. Phys. Soc. Jpn.* **55** 1294
[3] Medina A N, Hayashi M A, Cardoso L P, Gama S and Gandra F G 1998 *Phys. Rev. B* **57** 5900
[4] Rojas D P, Cardoso L P, Coelho A A and Gandra F G 2001 *Phys. Rev. B* **63** 165114
[5] Petrovic C, Bud'ko S L, Kogan V G and Canfield P C 2002 *Phys. Rev. B* **66** 054534
[6] Dickey R P, Freeman E J, Zapf V S, Ho P C and Maple M B 2003 *Phys. Rev. B* **68** 144402
[7] Sollie R and Schlottmann P 1991 *J. Appl. Phys.* **69** 5478, 2000 *ibit* **70** 5803
[8] Dommann A, Hulliger F, Ott H R and Gramlich V 1985 *J. Less-Common Met.* **110** 331
[9] Gignoux D, Schmitt D, Zerguine M, Ayache C and Bonjour E 1986 *Phys. Lett. A* **117** 145
[10] Palstra T T M, Menovsky A A, Nieuwenhuys G J and Mydosh J A 1986 *J. Magn. Magn. Mater.* **54-57** 435
[11] Menovsky A A, Snel C E, Gortenmulder T J, Tan H J and Palstra T T M 1986 *J. Crystal Growth* **74** 231
[12] Hiebl K, Horvath C, and Rogl P 1986 *J. Less-Common Met.* **117** 375
[13] Ayache C, Beille J, Bonjour E, Calemczuk R, Creuzet G, Gignoux D, Najib A, Schmitt D, Voiron J and Zerguine M 1987 *J. Magn. Magn. Mater*. **63 & 64** 329
[14] Gignoux D, Schmitt D and Zerguine M 1988 *Phys. Rev. B* **37** 9882
[15] Bhattacharjee A K, Coqblin B, Raki M, Forro L, Ayache C and Schmitt D 1989 *J. Physique* **50** 2781
[16] Steeman R A, Dirkmaat A J, Menvovsky A A, Frikkee E, Nieuwenhuys G J and Mydosh J A 1990 *Physica B* **163** 382
[17] Damas de Réotier P, Yaouanc A, Calemczuk R, Huxley A D, Marcenat C, Bonville P, Lejay P, Gubbens P C M and Mulders A M 1997 *Phys. Rev.* B **55** 2737
[18] Gignoux D, Schmitt D, Zerguine M and Murani A P 1988 *J. Magn. Magn. Mater.* **76 & 77** 401
[19] Tchoula Tchokonté M B, du Plessis P de V, Strydom A M and Kaczorowski D 2001 *J. Magn. Magn. Mater.* **226-230** 173
[20] Ragel F C, du Plessis P de V (2004), *J. Phys.: Condens. Matter* **16** 2647
[21] Tchoula Tchokonté M B, du Plessis P de V, Strydom A M 2005 *Solid State Comm*. **136** 450
[22] Bouziane K and du Plessis P de V (1999) *J. Phys.: Condens. Matter* **11** 3161
[23] Lavagna M, Lacroix C, and Cyrot M (1982) *Phys. Lett. A* **90** 210

[24] Lavagna M, Lacroix C and Cyrot M (1983) *J. Phys. F: Met. Phys*. **13** 1007
[25] Bellarbi B, Benoit A, Jaccard D, Mignot J M and Braun H F 1984 *Phys. Rev. B* **30** 1182
[26] Thompson J D, McElfresh M W, Willis J O, Fisk Z, Smith J L and Maple M B 1987 *Phys. Rev. B* **35** 48
[27] Kagayama T, Oomi G, Takahashi H, Mōri N, Ōnuki Y and Komatsubara T 1991 *Phys. Rev. B* **44** 7690
[28] Umeo K, Kadomatsu H and Takabatake T 1996 *Phys. Rev. B* **54** 1194
[29] Zheng-zhong Li and Yang Qiu 1991 *Phys. Rev. B* **43** 12906
[30] Wermbter S, Sabel K and Czycholl G 1996 *Phys. Rev. B* **53** 2528
[31] Aliev F G, Brant N B, Moshchalkov V V and Chudinov S M 1984 *J. Low Temp. Phys.* **57** 61
[32] Sumiyama A, Oda Y, Nagano H, Ōnuki Y, Shibutani K and Komatsubara T 1986 *J. Phys. Soc. Jpn.* **55** 1294
[33] Sengupta K and Sampathkumaran E V 2006 *J. Phys.: Condens. Matter* **18** L115
[34] Medina A N, Hayashi M A, Cardoso L P, Gama S, and Gandra F G 1998 *Phys. Rev.* ***B*** **57** 5900
[35] Yoshimori A and Kasai H 1986 *Solid State Comm.* **58** 259
[36] Mutou T 2001 *Phys. Rev. B* **64** 245102
[37] Lawrence J M, Graf T, Hundley M F, Mandrus D, Thompson J D, Lacerda A, Torikachvili M S, Sarrao J L and Fisk Z 1996 *Phys. Rev. B* **53** 12559
[38] Besnus M J, Kappler J P, Meyer A, Sereni J, Siaud E, Lahiouel R and Pierre J 1985 *Physica B* **130** 240
[39] Balster H, Ihrig H, Kockel A and Methfessel S 1975 *Z. Physik B* **21** 241
[40] Gratz E and Zuckermann M J 1982 *Handbook on the Physics and Chemistry of Rare Earths* vol 5, ed K A Gschneidner Jr and L Eyring (Amsterdam: Elsevier) p 117; and references therein
[41] Aléonard R and Morin P 1984 *J. Magn. Magn. Mater.* **42** 151
[42] Andrei N 1982 *Phys. Lett*. A**87** 299
[43] Schlottmann P 1983 *Z. Phys. B: Condensed Matter* **51** 223
[44] Evans S M M, Bhattacharjee A K and Coqblin B 1991 *Physica B* **171** 293
[45] Batlogg B, Bishop D J, Bucher E, Golding B Jr., Ramirez A P, Fisk Z, Smith J L and Ott H R 1987 *J. Magn. Magn. Mater* **63 & 64** 441
[46] Adroja D T, Rainford B D, Neville A J and Jansen A G M 1996 *Physica B* **223 & 224** 275
[47] Castro Neto A H and Jones B A 2000 *Phys. Rev. B* **62** 14975